Study of controllable inclusion addition methods in Al melt

Jiawei Yang[1], Sarina Bao[2], Shahid Akthar[3], Yanjun Li[1]
[1]Norwegian University of Science and Technology, Trondheim, NO-7491, Norway, Tel: +47--73594891, Fax: +47--73550203, Email: jiawei.yang@ntnu.no
[2]SINTEF Materials and Chemistry, Trondheim, N-7465, Norway
[3] Research and Development Karmøy, Norsk Hydro, Håvik, N-4265, Norway

Keywords: Inclusion addition, Contaminations, Aluminium, Oxide films

Abstract

Ceramic Foam Filtration (CFF) is a widely used technique to remove inclusions from aluminium melt. To ensure sufficient inclusions in the melt during the grain refiners/filtration interaction, inclusion addition methods, such as chips addition, powder addition, mechanical stirring, and wet up-gassing have been studied in this work. It is found that the addition of oxide causes the formation of irregularly shaped micropores in the cast samples. Chip addition is simple to conduct, introducing large amount and large size of oxide film contamination. The 6061 alloy chips were more helpful for inclusion contamination than that for commercial purity Al chips. This is due to the improved wettability by magnesium (Mg) content in the chips. The addition of oxide powder is difficult due to the poor wetting between oxide and Al matrix. Vortex created by mechanical stirring and pre-treatment of the powders improved the powder addition significantly. Wet up-gassing introduces pores and a large amount of dross based on the flow rate of the Ar gas.

Introduction

The inclusion removal technique such as filtration by Ceramic Foam Filter (CFF) has been studied extensively [1-11] in the past decades. It is well known that an addition of grain refiner particles in aluminium melt reduce the filtration efficiency of CFF. However, the underlying mechanism has been less understood. A deeper understanding of the filtration mechanism under the influence of grain refiners is important. As the first step, contamination of aluminum (Al) melt with controlled addition (type and amount) of inclusions is critical to obtain an in-depth understanding of inclusion behavior in the filtration process in the presence of grain refiners.

There are some works published regarding how to contaminate the Al metal with inclusions. Voigt et.al [12] reported a particle seeding process to produce Al master alloy for pilot filtration test. Alumina, spinel, mullite and silica powders larger than 20 µm were introduced into the Al melt with the help of a vortex created in a 10 kg crucible with a graphite rotor. Mg was added in the aluminium alloy to improve the wetting behavior between aluminium melt and inclusions in their work. However, the parameters as the rotation velocity, metal temperature, and feeding rate were not mentioned.

Surappa et.al [13] and Yang et.al [14] managed to add Al oxides into the melt through mechanical stirring to make Metal Matrix Composite (MMC). However, the feeding rate and rotation velocity were not given. Banerji et.al [15] added TiO_2 and ZrO_2 particles into the Al melt. They also mentioned that the Mg addition helped to improve the wetting by substantially reducing the liquid-vapor surface tension of the molten Al, hence, increasing the chance of oxide particle being introduced into the melt. They claimed that pre-treated oxide powders were easier to add into the melt. The pretreatment such as ultrasonic vibration aided cleaning of the oxides in acetone, decanting and preheating of the oxides was applied. These steps helped to clean and degas the oxide particles. Thus, the chemisorbed water in the form of surface hydroxyls at the surface of the oxide powders could be removed at temperatures around 100°C.

Fritzsch et.al [16] used the SiC reinforced A356 composite master alloy containing SiC particles to contaminate their aluminium melt for the filtration tests. These SiC particles were much easier to add compared to oxide particles due to their better wettability with the Al melt [17], even though SiC are not typical inclusions in alumnium.

To study the influence of oxide addition on the porosity development and the mechanical properties, Ludwig et. al [18] added 10, 25 and 50 wt.% turning chips into A356 Al melt, respectively, and cast in a mold, where melt temperature, hydrogen content, pouring temperature, and die temperature were carefully controlled. It was concluded that the oxide films addition would cause a large fraction of small pores.

Akhtar et.al [19] have used different up-gassing methods to study the porosity and pore morphology in a directionally solidified A356 alloy. They concluded that up-gassing with wood and Ar-water mixture is most efficient in comparison with Ar-10% H_2, and Ar-10% NH_3.

Thus, we can conclude from these literatures that it is hard to introduce Al oxide, which is one of the most popular inclusions in aluminium melt. In addition, it is even harder to control the addition amount .

In the present work, chips addition, powder addition, mechanical stirring, and wet up-gassing have been studied to introduce inclusions into the melt. The purpose is to make master alloys for the filtration test with controllable amount and inclusion types, such as Al oxide to evaluate filtration mechanisms for later experiments. The mechanical stirring may break up the top surface oxide layer of the melt and introduce them into the melt. Since those oxide layers are already in the Al on the halve side, they are supposed to be easier to stay in the melt. The advantages of wet up-gassing are that the critical parameters such as melt temperature, temperature of the gas, argon flow rate, and the up-gassing time could be well controlled.

Experimental

The experimental alloy used in this study was commercial purity aluminum (CP-Al) with chemical compositions shown in Table 1. Different methods to add inclusions were tested, including chip addition, oxide powder addition, stirring, and wet up-gassing. The details of the different tests are shown in Table 2, where totally 0.5 kg melt was used for test 1 and 1.5 kg for test 2-6. All melt treatments were conducted in a muffin furnace with the temperature set to 820 °C. The crucible containing inclusion contaminated melt was taken out from the furnace and cooled in the original crucible for test 1 or cast in Cu mold for the rest.

The powder was from Alfa Aesar® with a composition of 95% alumina and 5% silica. The particle size distribution of the powder scatters from around 0.5 µm to 300 µm. The Al chips were made from either CP-Al ingot or commercial AA6061 alloy by turning.

Table 1: Chemical composition of the CP-Al

Element	Composition wt.%
Si	0.06065
Fe	0.05830
Cu	0.00146
Mn	0.00089
Mg	0.00074
Al	~99.8

For test 1, the chips were melted together with CP-Al ingot in an alumina crucible coated with boron nitride at temperature of 800°C. A hand agitation was applied by using a carbon rod for approximately 2 minutes after they were completely melted.

Table 2: Experimental overview

Test nr.	Melt treatment	Temp. (°C)	Casting
1	+50 wt.% AA6061 Chips	760	Air cooling with crucible
2	+20 wt.% CP-Al Chips	775	Cast in Cu mold
3	+20 wt.% AA6061 chips	775	Cast in Cu mold
4	+20 wt.% AA6061 chips + 3 wt.% ($95\%Al_2O_3 \sim 5\%SiO_2$) Powder	775	Cast in Cu mold
5	+20 wt.% AA6061 chips + 3 wt.% ($95\%Al_2O_3 \sim 5\%SiO_2$) Powder Mechanical stirring	780	Cast in Cu mold
6	Wet Ar up-gassing (0.1 normal l/min and 1 normal l/min)	780	Cast in Cu mold

For test 2 and 3, after the melt of the Al, the chips were slowly introduced by a steel spoon. Thereafter, an agitation with a carbon rod was conducted for approximately 2 minutes.

For test 4, the alumina-silica powders were introduced slowly by the same spoon after the chips were added into the melt by agitation as in test 3. While adding the powders, the melt was continuously agitated by carbon rod. The feeding rate of powder is approximately 45g/min.

Test 5 has the same process as test 4, only stirred mechanically by an automatic rotator, instead of hand agitation, with a steel impeller as shown in Figure 1. The impeller stirred below the melt surface with an angle of approximately 30-50°, thus, a vortex was generated around the impeller. The chips were first introduced into the Al melt and then agitation was started by impeller. After the chips were completely melted, the powder was carefully fed into the center of the vortex with a feeding rate of 45 g/min. The stirring time was 10 minutes. After the stirring, the temperature dropped from 800 °C to 714 °C. The melt was heated up again and poured out at 780 °C.

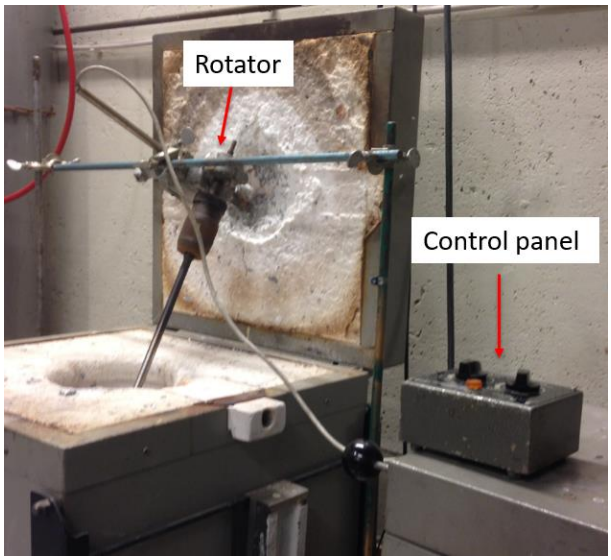

Figure 1: The auto rotator and muffin furnace involved in test 5

Two tests have been conducted in test 6. A humidity machine was attached to the crucible to add water vapor to the argon gas flushing, as shown in Figure 2. One of the humidifier inlets was connected to water bottle, while the other was connected to Ar gas, which was controlled by a flow meter with a flow rate of 0.1 and 1 normal L/min. The temperature for the wet gas outlet was set to 100 °C to ensure evaporation of the water. Then, wet Ar gas ran through a plastic pipe preheated to 110 °C to prevent condensation of the water. Afterward, the Ar gas ran through an alumina tube before it meets the melt. The alumina tube was dipped into the melt and wet Ar was flushed upward during the experiment from the bottom, thereof up-gassing. After up-gassing, a hand agitation with carbon rod was given to ensure the re-entry of oxidized surface layer into the melt.

After the experiments, all samples were cut, polished and characterized by Scanning Electron Microscope (SEM) and Energy-dispersive Spectroscopy (EDS).

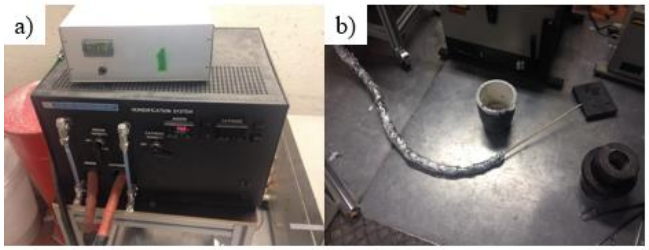

Figure 2: a) the humidity machine, and b) the alumina crucible involved in test 6

Results & Discussion

Test 1: CP-Al with 50 wt.% AA6061 chips

The crucible air cooled ingot from test 1 was sampled in the longitudinal section from top to the middle part. The microstructure characterized by SEM is shown in Figure 3. The chips were completely melted and mixed with the Al matrix. It shows that the top region of the ingot is packed with large amount of oxide films with length from approximately 100 µm to above 10 mm, and thickness approximately from 2 µm to 50 µm. As pointed out by Campbell [20], when the liquid metals are stirred or poured, the impinged films create a dry interface immersed in the bulk liquid and forms bifilms like in Figure 3 a). However, the region of 1.2 cm from the top and under was relatively clean. Only few pores and precipitates of Fe-Si intermetallic phase along the grain boundaries were observed. These films were added into the melt from chips with hand agitation. Due to the buoyancy force, most of the films floated up to the top region of the ingot during solidification.

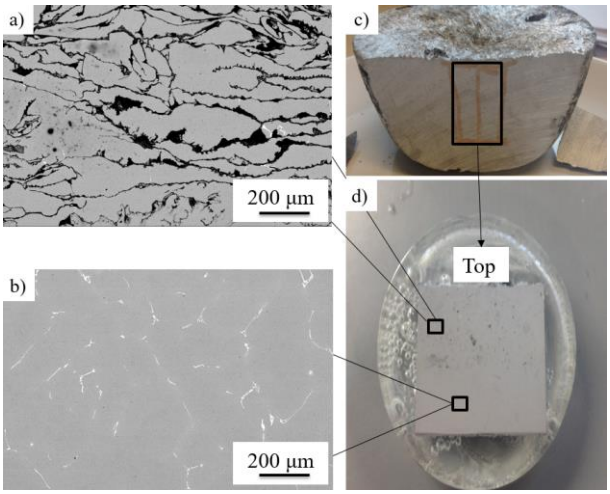

Figure 3: The CP-Al sample with 50% AA6061 chips addition in Test 1: The SEM figures from a) top and b) lower middle part of the ingot, c) the vertical cross-section of the crucible cooled ingot and d) its sampled area

Test 2: CP-Al with 20 wt.% CP-Al chips

20 wt.% CP-Al chips were melted with CP-Al ingot, and poured into the Cu-mold. As shown in Figure 4, oxide films up to 6 µm shown in the red circle, Fe-Si rich intermetallic phase as bright spot, and gray particles marked by blue arrows as SiC particles coming from grinding paper were observed in test 2. Micropores are observed in the whole cross-section of the cast sample, which is different from that in test 1. The micropores appear mostly in the top region than in the lower region. The sizes of the pores are approximately in the range of 0.5 µm to 20 µm. Ludwig et.al [18] had similar observation regarding pores formation after chips addition into the melt. The oxide films from the chips fold over dry side to dry side during the entrainment [20-22], which made micropores. This part of oxide films can be attributed to the high cooling rate of the casting sample in the copper mold. Thus, the oxide films did not

have enough time to float up, and they were relatively evenly trapped in the melt and formed micropores.

However, it may have no difference to filtrate this master alloy after re-melting. Ideally, all inclusions are supposed to be left inside the filter or sieved at the entrance of the filter, no matter where they were located inside the melt.

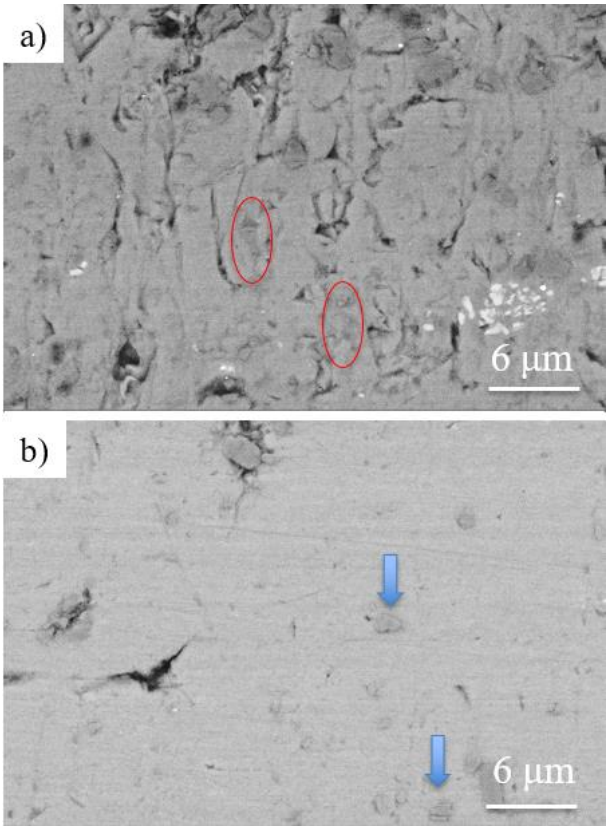

Figure 4: SEM figures for CP-Al with 20 wt.% CP-Al chips addition in Test 2 a) top region, and b) lower region. The blue arrow pointed the Si particles, and the red circles show the oxide films

Test 3: CP-Al with 20 wt.% AA6061 chips

As a comparison to the CP-Al chips, 20 wt.% AA6061 chips were used in this test. Large oxide films were observed at the top of the sample as shown in Figure 5. By using EDS, those oxide films were usually found to contain a very high percentage of Mg as shown in Figure 5 c). This indicates that Mg helps to increase the addition of aluminium oxide into the melt when compared to test 2. This can be explained as the wetting behavior between the matrix and the oxide films improved with Mg addition, as reported by different authors [1, 12, 15]. The Mg-containing chips are easier accepted by the melt than CP-Al chips. The oxide films are generally larger than that in test 2. Some pores and cracks occur at or around these films. As seen in previous tests, these films were observed in the top region. The rest of the sample is remained relatively clean, with some irregular micropores. As mentioned by Cambell [20], parts of the impinged surfaces contain entrapped air, forming the basis for the subsequent growth of porosity.

The benefit of adding chips is that the oxide films were readily introduced in an easy manner. Furthermore, the Mg-containing alloy chips have a better ability to keep oxide films in the melt. However, the distribution of the oxide films is still not very even, yet still better than test 1. In preparation tests, 0.5 kg Al with 20 wt. % chips were cast in Cu mold and a relatively even distribution of oxide films through the whole sample had been observed. This indicates that the cooling rate may be not high enough for this 1.5 kg of melt, so the oxide films still have time to float upward. No oxide particles, except the oxide films, were observed by chips addition, thereby, a powder addition has been tested in test 4 and 5.

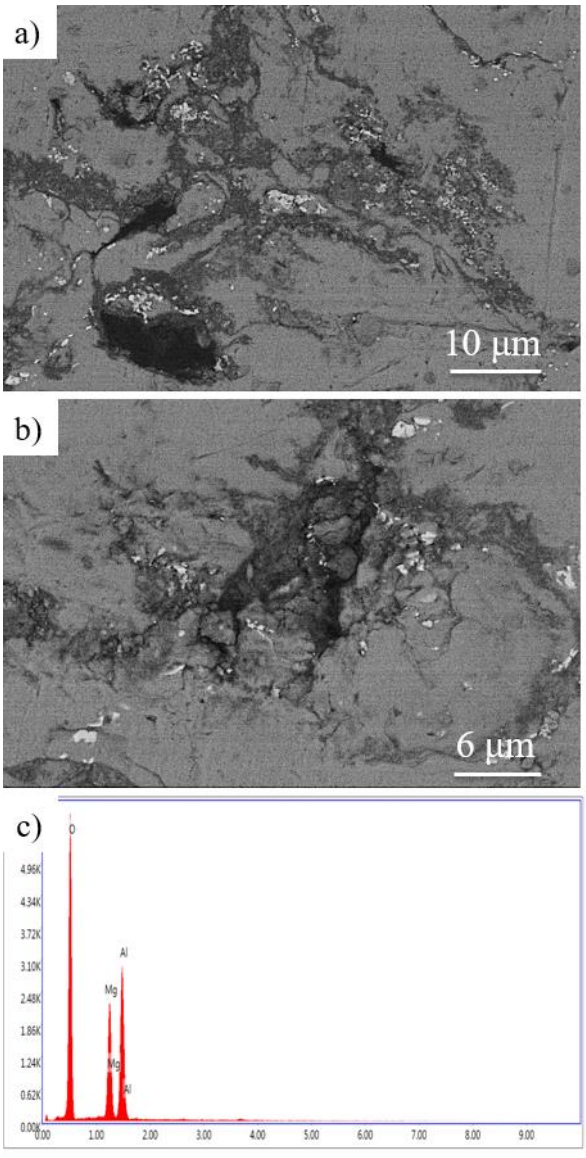

Figure 5: The oxide films in Test 3: a) SEM figures with 3000 magnification, b) 5000 magnification, and c) EDS result of oxide film in a)

Test 4: CP-Al with 20 wt.% AA6061 chips + 3 wt.% Alumina -Silica oxide powder

In addition to the chips, alumina-silica powders were introduced to the melt by hand agitation. As Figure 6 shows, the oxide particles were successfully introduced into the top 2 cm region of the ingot. These oxide particles are usually surrounded by the pores which can be observed by the naked eye and have a size of approximately 50 – 400 µm. Thus, some of the pores, without inclusions in, may be formed when the oxide particles get lost during the grinding and polishing process. The Mg-rich oxide films similar to that in Figure 5 were also found at the top region. The melt contains small irregular pores as other samples in the lower region.

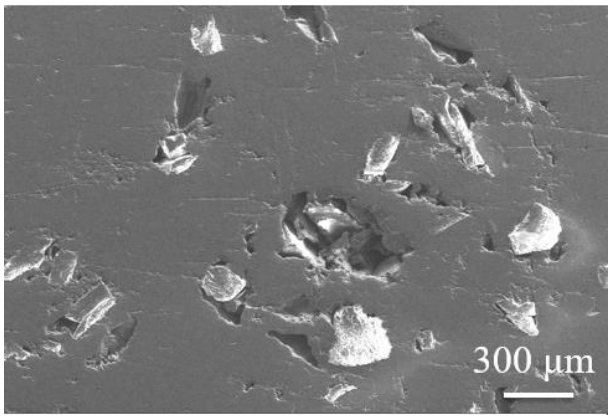

Figure 6: SEM figure of alumina particles in second electron beam mode near the top region of the ingot.

Test 5: CP-Al with 20 wt.% AA6061 chips + 3 wt.% Alumina -Silica oxide powder -Mechanical stirring

In test 5, mechanical stirring was used to help the introduction of oxide powders. Figure 7 shows the microscopic analysis of the cast sample. With the help of mechanical stirring, massive oxide powders were introduced. The distribution of the oxide particles was not limited at the top section anymore; even though the top section still has more particles than that in the lower region. The oxide particles in the top section seem to be easily wrapped together with the help of oxide films. The enveloped oxide film is not directly observed in the middle and lower region, but by EDS detection, it has approximately 7 wt.% Mg and 20 wt.% O surrounding the oxide particles, which suggested that particles are highly possible to be surrounded by the oxide films. By continuous stirring of the melt as shown in Figure 8, an amount of oxygen is introduced to the lower region of the melt due to the vortex. The oxide layer at the melt surface is easier to broke when the rotator is not perpendicular with the melt surface. The surface films were broken and trapped into the melt, and new oxide films are generated at the surface. Meanwhile, the surface oxide layer will fold together, and the dry side will wrap up the oxide particles and immerse into the melt. Thereby, the powders become easier to be introduced and more evenly distributed throughout the whole sample.

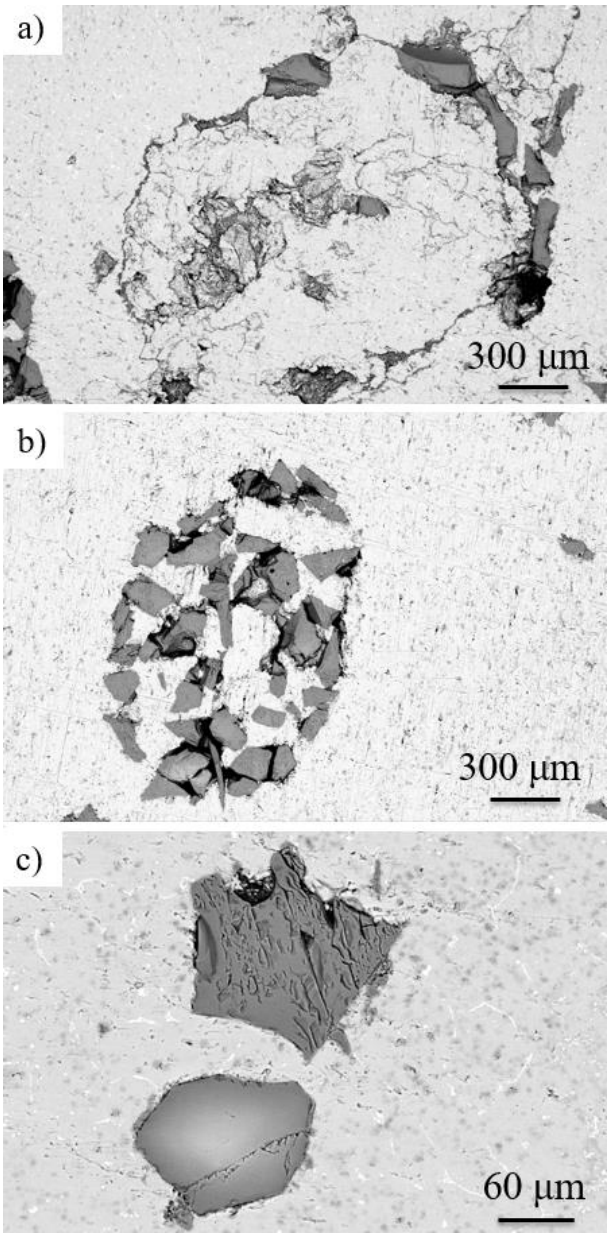

Figure 7: Mechanically stirred and cast sample in test 5: Microscopic view of the a) alumina particle surrounded by oxide films, b) agglomerated alumina particles, and c) alumina particles in the lower section

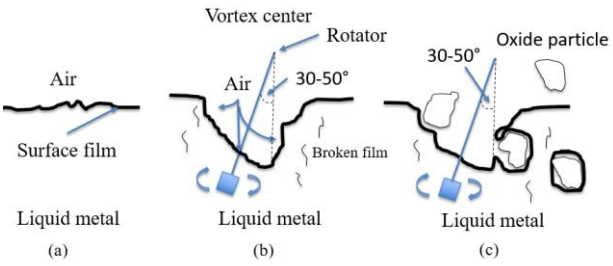

Figure 8: A sketch of stirring effect: a) before stirring, b) vortex is created, and broken films were introduced into

the melt and the air can reach to deeper part of the melt, and c) surface films envelope oxide particle and trapped them into the melt

With 10 minutes of stirring, there are still some powders remained in the crucible after pouring. However, by justifying experiment parameters such as tilt angle, rotation speed, rotation time etc., it is still possible to control the powder addition amount in the sample. Nevertheless, it is not so easy for the prediction for the film introduction.

Test 6: Wet Ar up-gassing

Wet Ar was flushed from the bottom of the melt in test 6. It is supposed to generate the alumina oxides contamination according to reaction 1

$$2Al(l) + 3H_2O\ (g) = Al_2O_3(s) + 3H_2(g) \quad (1)$$

It is expected that the likelihood of Al_2O_3 generated with the aluminium melt can be improved due to the wet bubbles.

Figure 9 shows the top section of the sample with 0.1 and 1 L/min wet Ar gas flushing. Some round pores are observed at the top region, similar to the typical gas defect. Irregularly shaped pores were also found after test 6 for both 1 and 0.1 normal L/min flow rate similar to Figure 4. For the 1 normal L/min sample, massive dross was formed during the up-gassing process. the generated films and particles were flushed up to the surface and became dross. This indicates that oxides are formed in the metal, even though no oxide particles were found in the sample. With a 0.1 normal L/min Ar flow rate in this test, small amount of dross was generated. It seems that pores are formed, and most of the oxides are collected as dross on top of the bulk metal. Thus, the force to flush up the oxide plus buoyancy force is larger than the gravity force of oxides. A wettable agent such as Mg can be a choice to keep inclusions in the melt. Meanwhile, the flow rate and the humidity rate of this test should be further controlled.

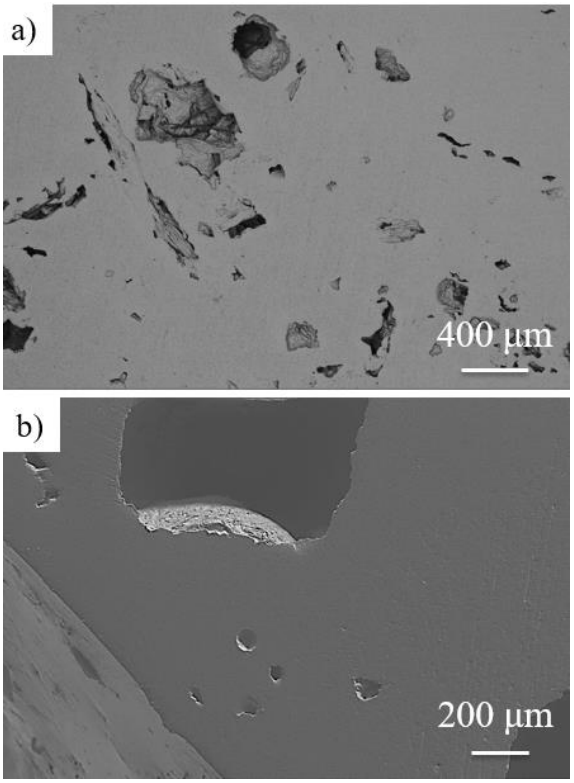

Figure 9: SEM figures for a) top section of 1 normal L/min wet Ar up-gassing sample, b) top section for 0.1 normal L/min wet Ar up-gassing sample in test 6.

Conclusions

Chips addition, oxide powder addition, mechanical stirring, and wet up-gassing were tested to introduce oxide inclusions into the Al melt in the present work. Following conclusions has been drawn from the course of this work.

- The inclusions were successfully added in the form of oxide films, pores, and oxide particles. It is still hard to control their amount and distribution.

- The chips addition is the easiest way to introduce oxide films. The AA6061 chips introduce more oxide contamination than that from CP-Al chips. This is because that Mg content in the chips improves the wettability between oxides and melts. In order to keep most of the oxide films evenly in the melt, fast cooling rate is necessary.

- The powder was successfully introduced by adding together with chips. Due to the poor wetting between oxide particles and Al matrix, a wettable agent such as Mg is necessary to be present for improving the wettability. Vortex in the melt aided by mechanical stirring can enhance the addition of oxide particles into the melt significantly.

- The wet up-gassing method could introduce Al oxide films into the melt, but not oxide particles.

- A combination of chips addition, powder addition and mechanical stirring get the best results among all tests so far.

Future work

- It is important to increase the wettability between oxide inclusions and the melt for contamination. Ni coated alumina powders can be a good solution in the future work.

- For the mechanical stirring, the parameters such as tilted angle, rotation speed and time, and temperature should be further optimized in future work with larger scale test.

- For the wet up-gassing, an optimization of the gas flow rate and water vapor rate is important to create and keep most of the oxide films in the melt. In addition, a wettable agent like Mg is also necessary.

Acknowledgment

This research was carried out as part of the Norwegian Research Council (NRC) - funded BIA-IPN Project (256724/O20) SmartAl. It includes the following partners: Hydro Aluminium AS, Hydal Aluminium Profiler AS, Hycast AS, Ekornes ASA, NTNU and SINTEF. Funding by the industrial partners and NRC is gratefully acknowledged. Thanks are also given to Emeritus Professor Lars Arneberg, and Research Scientist Martin Syvertsen for their useful advice and help.

References

1. Bao, S., *Filtration of aluminium-experiments, wetting and modelling*. 2011. 204 s.
2. Syvertsen, M. and S. Bao, *Performance Evaluation of Two Different Industrial Foam Filters with LiMCA II Data.* Metallurgical and Materials Transactions B, 2015. **46**(2): p. 1058-1065.
3. Bao, S., et al., *Inclusion (particle) removal by interception and gravity in ceramic foam filters.* Journal of Materials Science, 2012. **47**(23): p. 7986-7998.
4. Zhou, M., et al., *Deep filtration of molten aluminum using ceramic foam filters and ceramic particles with active coatings.* Metallurgical and Materials Transactions A, 2003. **34**(5): p. 1183-1191.
5. Buchilin, N.V., V.G. Maksimov, and V.G. Babashov, *Ceramic Filters for Aluminum Melt (Review).* Glass and Ceramics, 2015. **72**(7): p. 246-252.
6. Gauckler, L.J., et al., *Ceramic Foam For Molten metal Filtration.* JOM, 1985. **37**(9): p. 47-50.
7. Kennedy, M.W., et al., *Characterization of Ceramic Foam Filters Used for Liquid Metal Filtration.* Metallurgical and Materials Transactions B, 2013. **44**(3): p. 671-690.
8. Voigt, C., et al., *Effect of the filter surface chemistry on the filtration of aluminum.* Metallurgical and Materials Transactions B, 2015. **46**(2): p. 1066-1072.
9. Apelian, D. and R. Mutharasan, *Filtration: A Melt Refining Method.* JOM, 1980. **32**(9): p. 14-19.
10. Ray, S., B. Milligan, and N. Keegan, *Measurement of filtration performance, filtration theory and practical applications of ceramic foam filters.* Aluminium Cast House Technology, 2005: p. 1-12.
11. Damoah, L.N.W. and L. Zhang, *Removal of Inclusions from Aluminum Through Filtration.* Metallurgical and Materials Transactions B, 2010. **41**(4): p. 886-907.
12. Voigt, C., et al., *Filtration Efficiency of Functionalized Ceramic Foam Filters for Aluminum Melt Filtration.* Metallurgical and Materials Transactions B, 2017. **48**(1): p. 497-505.
13. Surappa, M.K., S.V. Prasad, and P.K. Rohatgi, *Wear and abrasion of cast Al-Alumina particle composites.* Wear, 1982. **77**(3): p. 295-302.
14. Jingyu, Y. and D.D.L. Chung, *Wear of bauxite-particle-reinforced aluminum alloys.* Wear, 1989. **135**(1): p. 53-65.
15. Banerji, A. and P.K. Rohatgi, *Cast aluminium alloy containing dispersions of TiO2 and ZrO2 particles.* Journal of Materials Science, 1982. **17**(2): p. 335-342.
16. Fritzsch, R., et al., *Electromagnetic Priming of Ceramic Foam Filters (CFF) for Liquid Aluminum Filtration*, in *Light Metals 2013*, B.A. Sadler, Editor. 2016, Springer International Publishing: Cham. p. 973-979.
17. Bao, S., et al., *Wetting of pure aluminium on graphite, SiC and Al2O3 in aluminium*

filtration. Transactions of Nonferrous Metals Society of China, 2012. **22**(8): p. 1930-1938.
18. Ludwig, T., et al., *Influence of Oxide Additions on the Porosity Development and Mechanical Properties of A356 Aluminium Alloy Castings.* International Journal of Metalcasting, 2012. **6**(2): p. 41-50.
19. Akhtar, S., et al., *A Comparative Study of Porosity and Pore Morphology in a Directionally Solidified A356 Alloy*. International Journal of Metalcasting, 2009. **3**(1): p. 39-52.
20. Campbell, J., *The consolidation of metals: the origin of bifilms*. Journal of Materials Science, 2016. **51**(1): p. 96-106.
21. Campbell, J., *Chapter 2 - Entrainment*, in *Castings (Second Edition)*, J. Campbell, Editor. 2003, Butterworth-Heinemann: Oxford. p. 17-69.
22. Gopalan, R. and N.K. Prabhu, *Oxide bifilms in aluminium alloy castings–a review*. Materials Science and Technology, 2011. **27**(12): p. 1757-1769.